運動野、前運動野、視床、島、後帯状回に脳活動がみられることを指摘している。これらの脳部位は今回の我々の研究で明らかとなった脳活動部位と類似しており、腰痛をイメージするい画像を視認しただけでも腰痛経験者では腰痛を経験してしまうことが示唆された。

F. 健康危険情報
特になし。

G. 研究発表
学会発表
下和弘ら:「腰痛経験者では視覚情報によって腰痛が惹起されるか？—Virtual low back pain stimuli activates cortical representation of emotions in person with nonspecific low back pain.」日本臨床神経生理学会、 2010、 神戸

下和弘ら:「腰痛の診断、治療法に関する研究：痛み・しびれの可視化技術の確立並びにMRIを用いた脊髄投射路及び末梢神経イメージング法の確立」研究事業の成果報告会、 2011、 東京

論文発表
該当なし

H. 知的財産権の出願・登録状況
該当なし

I. 知的財産権の出願・登録状況
該当なし

厚生労働省科学研究費補助金（長寿科学総合研究事業）
分担研究報告書

腰痛の診断、治療法に関する研究：痛み・しびれの可視化技術の確立並びに、MRIを用いた脊髄投射路及び末梢神経イメージング法の確立に関する研究

研究分担者　紺野慎一　福島県立医科大学医学部整形外科学講座　教授

研究要旨：慢性腰痛患者の脳活動を解析するために、慢性腰痛患者と正常ボランティアの２群を対象とした。腰部を圧迫刺激時に、脳functional-MRIを撮影し、脳不活部位を２群間で比較した。慢性腰痛患者の脳賦活部位は、後帯状皮質でも認められ、腰痛を不快感の強い痛みと感じていることが示唆される。また、fMRIは客観的評価法の１つになりうる可能性が示唆される。

A. 研究目的

難治性の非特異的腰痛患者において、心理的・社会的問題の関与がリスク因子として指摘されており、脳の情動的な認知の違いにより個人の感じる疼痛に違いが生じることが知られている。本研究では、脳 functional-MRI を用いて、慢性腰痛患者における疼痛関連脳活動の特徴を明らかにすることを目的とした。

B. 研究方法

シリーズ１：対象者毎に圧迫力を設定
慢性腰痛患者 8 名と正常ボランティア 8 名を対象とした。腹臥位とし、第 4、5 腰椎椎間で正中から 5cm 左外側に、シリンジを用いて圧迫刺激した。撮像前に、圧迫刺激の程度を visual analogue scale（VAS）30mm と 50mm の痛み刺激に設定し、撮像時の刺激に対する痛みと不快感をVASで記録した。fMRI撮影時に、ブロック型パラダイム法で、圧迫タスクを３０秒間、その後３０秒間の安静期を設け、3 回タスクを繰り返した。

シリーズ２：慢性腰痛患者６名と正常ボランティア７名を対象とした。圧迫部位は、シリーズ１と同様で、圧迫力は、統一した圧迫力（300kPa, 400kPa, 500kPa）に設定し、ブロック型パラダイム法で行った。

MRIは、3.0テスラ高速MRIスキャナーを使用した。高速エコープランナー法による脳のT2強調MRIスキャンを行い、解析ソフトウェアBrain voyagerを用いて、血中酸素濃度依存的（BOLD）信号を解析した。

本研究は、当該研究施設の倫理委員会にて承認されている。対象者の人権擁護として、研究の承諾の取り消しはいつでも行うことができる。対象者の不利益を一

切被らない。個人情報を保護するために、匿名化したデータで解析を行う。以上の内容を含む研究参加説明書を用いて、研究内容を説明し、研究参加への承諾を得た。

C. 研究結果

シリーズ１：慢性腰痛患者では、脳賦活は、正常ボランティアと比較して、後帯状皮質に特異的に認められた。
シリーズ２：圧迫の強さに従って、対象者の感じる疼痛の強さが有意に強くなった。しかし、２群間で差が認められなかった。慢性腰痛患者の後帯状皮質でのBOLD信号は、健常者と比較して、有意に増大した。

D. 考察

本研究の結果から、慢性腰痛患者では、圧迫刺激に対して、不快感の強い腰痛を感じていることが示唆された。さらに、感じてる疼痛の程度が同じであっても、慢性腰痛患者では、脳賦活が増大していることから、fMRIが客観的評価法の１つになりうる可能性が示唆された。

E. 結論

後帯状皮質が、慢性腰痛患者で特異的な脳賦活部位であると考えられる。腰痛の治療による反応性についての検討に有用である。

F. 健康危険情報

総括研究報告書に記載

G. 研究発表

１．論文発表

該当なし

２．学会発表

該当なし

H. 知的財産権の出願・登録状況

該当なし

厚生労働科学研究費補助金（長寿科学総合研究事業）
分担研究報告書

腰痛の診断、治療法に関する研究：痛み・しびれの可視化技術の確立並びに、MRIを用いた脊髄投射路及び抹消神経イメージング法の確立に関する研究

腰椎変性疾患における椎間運動パターンの解明に関する研究

研究分担者　岩﨑幹季　長本行隆　藤森孝人　菅本一臣　大阪大学整形外科

研究要旨：大阪大学整形外科では以前から 3D-MRI を用いたボリュームレジストレーション法（以下 VR 法）を用いて正常頚椎、腰椎の生体内 3 次元運動解析を報告してきた。本手法では、従来の modality では限界のあった生体腰椎の微細な椎間運動を 3 次元的かつ高精度で捉えることができる。今回本手法をさらに解析精度の向上が見込める CT に適応して、腰椎変性疾患の運動解析を行い、正常腰椎との比較により変性腰椎の椎間運動パターンを見出し、腰椎異常可動性の新たな評価や病態の解明、早期診断法の確立を目指す。

A. 研究目的

腰椎変性疾患や腰椎手術後などに生じる腰椎椎間異常可動性を高精度な手法で 3 次元計測し、正常腰椎との動態の比較を行うことで可能であればこれを明確に定義し、さらに臨床症状との関連性についても調査すること。

B. 研究方法

腰椎変性疾患で固定術を予定している 20 例を対象とする。臨床評価パラメータとして術前と術後 6 カ月に神経学的所見、JOA スコア、腰痛、下肢症状の有無について調査する。CT 撮影は中間位、最大前後屈位、最大両回旋位の 5 ポジションで行い（図 1）、PC ソフトウェアによる画像解析処理（VR 法）により腰椎椎間運動の 3 次元解析を行う。

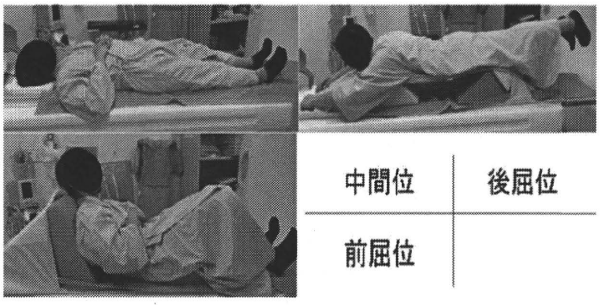

図 1

動作解析に関しては、術前の罹患変性椎間や術後の隣接椎間における正常動態との相違に注目する。各評価パラメータと椎間可動域との関連性についても検討を行う。

（倫理面への配慮）

①撮影により脊椎由来の症状が悪化する危険性への対策として、全撮影に必ず

分担研究者が立会い、症状の変化に注意を払いながら撮影を行うこととし、症状に異変を生じた場合は速やかに撮影を中止する。

②X 線被曝の問題。治療上 CT 撮影の必要な症例のみを対象としており、複数回の撮影でも中間位以外では撮影線量を 1/5 に低減して全被曝量の増加を抑えるようにしている。

（CT を用いた VR 法の動作解析精度）
新鮮凍結ブタの脊椎を用いて動作解析手法の精度を検証した（図２）。

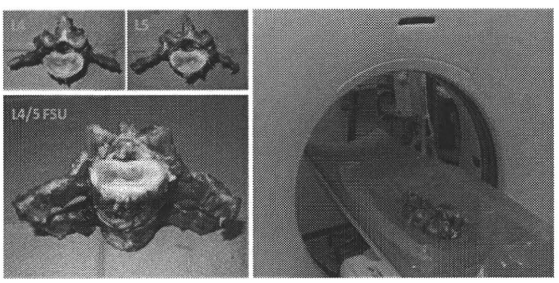

図２

ブタ L4, L5 椎体を用いて、各骨内に tantalnum ball を 8 個打ちこみ CT を撮影、marker-based registration により得られた値を正解値として、8 種類の椎間動作を VR 法による測定値と比較し、その誤差を RMSd として算出した。表１の如く非常に高い精度が得られた。

RMSd	Rx	Ry	Rz	Tx	Ty	Tz
	0.07°	0.01°	0.07°	0.02mm	0.06mm	0.13mm

表１

C. 研究結果

現在、画像取得症例は 22 例である。疾患内訳は、変性すべり症 14 例、分離すべり症 3 例、変性側弯 2 例、腰部脊柱管狭窄症 1 例、腰椎固定術後隣接椎間障害 2 例である。さらに、術後 6 カ月時の画像取得まで終了した症例は 8 例である。動作解析は 6 例で終了し、うち 4 例は術前後の動作解析が終了した。解析済みの症例を以下に供覧する。

1. 変性椎間の解析
L4 変性すべり 6 例の L4/5 椎間（罹患椎間）の可動域を表２に示す。

症例	前後屈(°)	片側回旋(°)
1	6.1	4.0
2	2.3	1.5
3	13.4	6.2
4	12.8	2.0
5	13.9	3.0
6	14	4.0
平均	10.4	3.5

表２

我々が以前報告した健常腰椎の回旋可動域計測では L4/5 片側回旋可動域は 1.7±0.6°であるのに対し、L4/5 すべり椎間では平均 3.5°と回旋可動域は増加する傾向が認められた。

2. 腰椎固定術前後の固定隣接椎間の動態変化

腰椎固定術を行った 4 症例に関しては、固定隣接上下椎間の術前後の動態変化に焦点を絞り、結果を以下に供覧する。椎間可動域変化率は、⊿(%)=(術前°-術後°) / 術前° × 100 と定義して算出した。

表３　固定隣接上位椎間における術前後可動域変化

	疾患	術式	固定隣接上位椎間変化率				
				前後屈		回旋	
1	L4変性すべり	L4/5 PLIF	L3/4	10.3°	→11.4°	0.2°	→0.6°
2	L4変性すべり	L4/5 PLIF	L3/4	11.7°	→12.4°	2.5°	→1.9°
3	L4分離すべり	L4/5 PLIF	L3/4	4.1°	→10.7°	1.4°	→1.0°
4	L4変性すべり	L4/5 PILF + L3/4 PLF	L2/3	5.4°	→14.0°	0.9°	→1.1°

表４　固定隣接下位椎間における術前後可動域変化

	疾患	術式	固定隣接下位椎間変化率				
				前後屈		回旋	
1	L4変性すべり	L4/5 PLIF	L5/S	15.0°	→13.2°	0.6°	→1.8°
2	L4変性すべり	L4/5 PLIF	L5/S	4.5°	→11.5°	1.3°	→1.2°
3	L4分離すべり	L4/5 PLIF	L5/S	6.3°	→12.5°	0.5°	→0.8°
4	L4変性すべり	L4/5PLIF + L3/4 PLF	L5/S	0.1°	→1.8°	0.2°	→0.4°

隣接上下椎間では、前後屈運動、回旋運動ともに概して術後には可動域が増加する傾向を認めた（表３，４）。

D. 考察

CT を用いた VR 法では非常に高い精度で椎間運動の 3 次元的動態の計測ができ、かつアニメーションによる動態の可視化により質的評価も可能である。これまで腰椎疾患や腰椎手術例などの病的な椎間に対する生体内 3 次元動態解析はこれまでほとんどな報告がなく、このような背景において今回初めて腰椎変性疾患に対する治療介入前後の生体内 3 次元動態変化を捉えることに成功した。

腰椎固定手術後の隣接椎間障害については多くの報告があり、Park らの review によれば、腰椎固定術後、隣接椎間に変性所見の出現・増強などの画像所見が認められる頻度は 5.2%~100%であり、隣接椎間への追加手術の頻度は 0~27.5%と報告されている[1]。生体力学的な研究でも、椎間固定による可動椎間減少によりその隣接上下椎間に可動性亢進などの変化をきたすことが示されている[2]。そしてこの可動性の変化は、インストルメントの長さや剛性の高さに比例する[3]と報告されている。本研究でも隣接上下椎間の可動域は概して増加する傾向を認め、今後解析症例を増やして固定椎間の長さの違いによる隣接椎間可動性変化の相違についても検討を加える。また Okuda らは L4/5 PLIF の術後症例において、隣接上位椎体椎弓の傾きや隣接上位椎間関節の関節面角度左右差が大きいことを隣接上位椎間障害の危険因子として明らかにしているが[4,5]、今回隣接上位椎間において回旋、前後屈ともに可動性が増加している症例も認められ、隣接上位椎間における前後屈、回旋各可動域増加が隣接椎間障害に関与していると推察している。

最近、腰椎固定術後の仙腸関節障害についても報告されている[6-8]。これも一種の隣接関節障害と考えられているが、そもそも可動域のほとんど認められない仙腸関節に生じる動態変化を証明した報告は過去にない。我々は先行研究として腰椎運動に伴う正常仙腸関節の生体内における動きや腰椎変性疾患患者との動態の相違について検討しており、正常仙腸関節では腰椎運動に伴う動きはほとんど認められないこと、また腰椎変性疾患群では有意に仙腸関節の可動性が亢進していることを生体内 3 次元解析により明らかにし（下図）、腰椎疾患群におけるこのような仙腸関節の可動性亢進は、高齢者における腰痛の一因となっているのではないかと推察している。そこで、これらの腰椎変性疾患患者の中で腰椎固定術例に関しては、術後の仙腸関節の動態変化についても検討を行い、今後腰椎固定術後の仙腸関節障害の病態についても生体力学的観点から明らかにしたいと考えている。

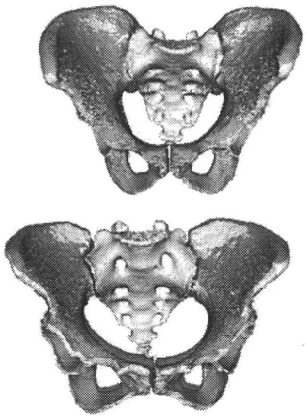

正常仙腸関節（右）と腰椎疾患仙腸関節（左）の動き

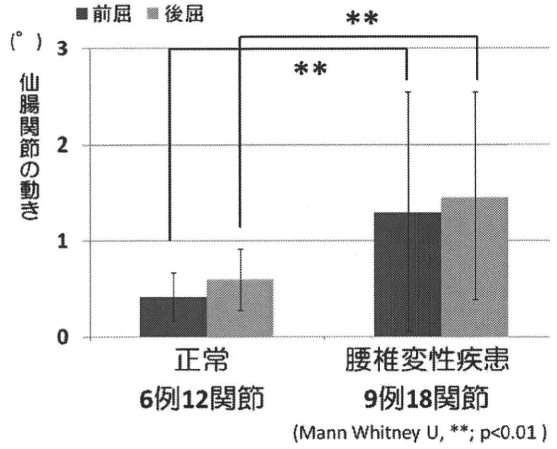

本手法の限界として、①腰椎可動域の再現性の問題：治療介入後の動態変化を捕捉するには、本来ならば一定可動域内における動態を比較することが望ましい。しかし、腰椎では体表からのランドマークが少なく、装具などで腰椎運動を規定しても、腰下肢痛の状態、患者の意欲、装具のフィッティングの状態などの影響を受け、高い再現性をもって一定の可動域を作ることが困難である。このため腰椎運動に関しては角度による評価ではなく、全腰椎運動に対する各椎間の寄与率で評価することも検討している。②撮影範囲の問題：前屈位での撮影では、体幹～頭部がCTの筐体に接触し、上位腰椎の撮影範囲はかなり患者の体格や姿勢により変化してしまう。などがあげられる。

E. 結論

VR法により腰椎固定術後の隣接椎間や仙腸関節に生じる生体内3次元動態変化を捉えることに成功した。

参考文献

1. Maigne JY, Planchon CA. Sacroiliac joint pain after lumbar fusion. A study with anesthetic blocks. Eur Spine J. 2005;14:654-8.
2. Park P, Garton HJ, Gala VC et al. Adjacent segment disease after lumbar or lumbosacral fusion: Review of the literature. Spine 2004; 29:1938-44
3. Panjabi M, Henderson G, Abjornson C et al. Multidirectional testing of one- and two-level ProDisc-L versus simulated fusions. Spine 2007;32:1211-19
4. Okuda S, Iwasaki M, Miyauchi A, Aono H, Morita M, Yamamoto T. Risk factors for adjacent segment degeneration after PLIF. Spine 2004 15;29:1535-40.
5. Okuda S, Oda T, Miyauchi A, Tamura S, Hashimoto Y, Yamasaki S, Haku T, Kanematsu F, Ariga K, Ohwada T, Aono H, Hosono N, Fuji T, Iwasaki M. Lamina horizontalization and facet tropism as the risk factors for adjacent segment degeneration after PLIF. Spine 2008;33:2754-8.
6. Shono Y, Kaneda K, Abumi K et al. Stability of posterior spinal instrumentation and its effects on adjacent motion segments in the lumbosacral spine. Spine 1998;23:1550-8
7. Ha KY, Lee JS, Kim KW. Degeneration of sacroiliac joint after instrumented lumbar or lumbosacral fusion: a prospective cohort study over five-year follow-up. Spine 2008;33:1192-8.
8. Katz V, Schofferman J, Reynolds J. The sacroiliac joint: a potential cause of pain after lumbar fusion to the sacrum. J Spinal Disord Tech. 2003;16:96-9.

F. 健康危険情報
総括研究報告書に記載

G. 発表

1. 論文発表：
Nagamoto Y, Ishii T, Sakaura H, Iwasaki M, Morimoto H, Kashii M, Yoshikawa H, Sugamoto K. In vivo three-dimensional kinematics of the cervical spine during head rotation in patients with cervical spondylosis. Spine 36 (in press), 2011

2. 学会発表：
1. Nagamoto Y, Ishii T, Sakaura H, Iwasaki M, Moritomo H, Kashii M, Sugamoto K, Yoshikawa H. *In vivo* three-dimensional kinematics of the cervical spine during head rotation in patients with degenerative cervical spine. 56th Annual meeting of the Orthopaedic Research Society (New Orleans, Louisiana, Mar., 2010)
2. 長本行隆、西井孝、坂浦博伸、藤森孝人、岩崎幹季、菅本一臣、吉川秀樹：腰部神経根の 3 次元イメージングの試み：外側病変診断における有用性　第 39 回日本脊椎脊髄病学会（平成 22 年 4 月高知）
3. 長本行隆、藤森孝人、柏井将文、岩崎幹季、菅本一臣、吉川秀樹：仙腸関節の生体内三次元動態解析：第 25 回日本整形外科学会基礎学術集会（平成 22 年 10 月京都）
4. Nagamoto Y, Fujimori T, Sakaura H, Kashii M, Iwasaki M, Yoshikawa H, Sugamoto K. In vivo three-dimensional kinematics of the iliosacral joint induced by trunk motion using low-dose CT volme registration method. 57th Annual Meeting of the Orthopaedic Research Society (Long Beach, California, Jan., 2011)

H. 財産健の出願・登録状況

1. 特許取得：未取得
2. 実用新案登録：未取得
3. その他：特になし

III. 研究成果の刊行に関する一覧表

研究成果の刊行に関する一覧表

雑誌

発表者氏名	論文タイトル名	発表誌名	巻号	ページ	出版年
Shibata S, Yasuda A, Renault-Mihara F, Suyama S, Katoh H, Inoue T, Inoue YU, Nagoshi N, Sato M, Nakamura M, Akazawa C, Okano H.	Sox10-Venus mice: a new tool for real-time labeling of neural crest lineage cells and oligodendrocytes.	Mol Brain.	3(1)	31	2010
Mukaino M, Nakamura M, Yamada O, Okada S, Morikawa S, Renault-Mihara F, Iwanami A, Ikegami T, Ohsugi Y, Tsuji O, Katoh H, Matsuzaki Y, Toyama Y, Liu M, Okano H.	Anti-IL-6-receptor antibody promotes repair of spinal cord injury by inducing microglia-dominant inflammation.	Exp Neurol.	224	403-414	2010
Takahashi Y, Tsuji O, Kumagai G, Hara CM, Okano HJ, Miyawaki A, Toyama Y, Okano H, Nakamura M.	Comparative study of methods for administering neural stem/progenitor cells to treat spinal cord injury in mice.	Cell Transplant.	in press.		
Tsuji O, Miura K, Okada Y, Fujiyoshi K, Mukaino M, Nagoshi N, Kitamura K, Kumagi G, Nishino M, Tomisato S, Higashi H, Nagai T, Katoh H, Kohda K, Matsuzaki Y, Yuzaki M, Ikeda E, Toyama Y, Nakamura M, Yamanaka S, Okano H.	Therapeutic potential of appropriately evaluated safe-induced pluripotent stem cells for spinal cord injury	PNAS	107	12704 -12709	2010

Munehisa Shinozaki, Yuichiro Takahashi, Masahiko Mukaino, Nobuhito Saito, Yoshiaki Toyama, Hideyuki Okano, and Masaya Nakamura.	Novel Concept of Motor Functional Analysis for Spinal Cord Injury in Adult Mice.	Journal of Biomedicine and Biotechnology.	In Press	Article ID	2011
Nagamoto Y, Ishii T, Sakaura H, Iwasaki M, Morimoto H, Kashii M, Yoshikawa H, Sugamoto K.	In vivo three-dimensional kinematics of the cervical spine during head rotation in patients with cervical spondylosis.	Spine	36 (in press)		2011
岡野栄之、辻収彦、三浦恭子、岡田洋平、藤吉兼浩、高木岳彦、金子慎二郎、戸山芳昭、山中伸哉、中村雅也	中枢神経系と末梢神経系の再生戦略.	Peripheral Nerve 末梢神経	21	145-151	2010
藤吉兼浩、疋島啓吾、辻収彦、戸山芳昭、岡野栄之、中村雅也	拡散テンソル tractography	脊椎脊髄ジャーナル	24(3)	315-323	2010
辻収彦，名越慈人，藤吉兼浩，戸山芳昭，岡野栄之，中村雅也.	脊髄損傷に対するiPS細胞および神経堤幹細胞移植	脊椎脊髄	23	818-827	2010
三浦恭子，辻収彦，岡野栄之	.iPS細胞の安全性の担保.	再生医療	9	315-322.	2010
辻収彦，中村雅也，岡野栄之	iPS細胞を利用した神経再生	細胞	11月号	16−19	2010
熊谷玄太郎、岡田洋平、藤哲、戸山芳昭、中村雅也、岡野栄之.	脊髄損傷に対するＥＳ細胞由来神経幹細胞ー移植.	脊椎脊髄ジャーナル.	123	835-845	2010
Kyoko Miura,Osahiko Tsuji,Masaya Nakamura and Hideyuki Okano	Toward using iPS cells to treat spinal cord injury:Their safety and therapeutic efficacy	Inflammation and Regeneration	31(1)	2-10	2011

IV. 研究成果の刊行物・別刷

Shibata *et al. Molecular Brain* 2010, **3**:31
http://www.molecularbrain.com/content/3/1/31

Molecular Brain

RESEARCH Open Access

Sox10-Venus mice: a new tool for real-time labeling of neural crest lineage cells and oligodendrocytes

Shinsuke Shibata[1], Akimasa Yasuda[1,2], Francois Renault-Mihara[1,2], Satoshi Suyama[1], Hiroyuki Katoh[1,2,3], Takayoshi Inoue[4], Yukiko U Inoue[4], Narihito Nagoshi[1,2,3], Momoka Sato[1,2], Masaya Nakamura[2], Chihiro Akazawa[5], Hideyuki Okano[1*]

Abstract

Background: While several mouse strains have recently been developed for tracing neural crest or oligodendrocyte lineages, each strain has inherent limitations. The connection between human *SOX10* mutations and neural crest cell pathogenesis led us to focus on the *Sox10* gene, which is critical for neural crest development. We generated *Sox10*-Venus BAC transgenic mice to monitor Sox10 expression in both normal development and in pathological processes.

Results: Tissue fluorescence distinguished neural crest progeny cells and oligodendrocytes in the *Sox10*-Venus mouse embryo. Immunohistochemical analysis confirmed that Venus expression was restricted to cells expressing endogenous Sox10. Time-lapse imaging of various tissues in *Sox10*-Venus mice demonstrated that Venus expression could be visualized at the single-cell level *in vivo* due to the intense, focused Venus fluorescence. In the adult *Sox10*-Venus mouse, several types of mature and immature oligodendrocytes along with Schwann cells were clearly labeled with Venus, both before and after spinal cord injury.

Conclusions: In the newly-developed *Sox10*-Venus transgenic mouse, Venus fluorescence faithfully mirrors endogenous Sox10 expression and allows for *in vivo* imaging of live cells at the single-cell level. This *Sox10*-Venus mouse will thus be a useful tool for studying neural crest cells or oligodendrocytes, both in development and in pathological processes.

Background

The neural crest (NC) is a transient embryonic tissue. NC cells delaminate from the dorsal neural tube as it closes [1] and migrate to distinct locations, where they differentiate into various cell types, including neurons, glia, melanocytes, endocrine cells, and mesenchymal cells [2-5].

The Sox proteins belong to the HMG (high mobility group) domain of transcription factors [6,7]. Sox-E is the earliest marker of a subset of cells at the border of the neural plate that will give rise to NC-lineage cells [8]. Sox10, which is a member of the Sox-E family and shares high sequence homology with other Sox-E member transcription factors, regulates and coordinates diverse developmental processes such as organ development and cell survival and specification. Sox10 is highly expressed in the emerging NC and later in the developing glial cells of the peripheral nervous system (PNS) and central nervous system (CNS) [9,10]. Whether in mice or humans, Sox family protein deletions or mutations often result in developmental defects and congenital disease, and mutations of the human *SOX10* gene are associated with NC cell abnormalities [9,11-13].

Several transgenic mouse strains dedicated to tracing the NC lineage have already been developed, such as *Wnt1*-Cre [14], *Protein zero (P0)*-Cre [15], and *Ht-PA*-Cre [16] mice crossed with Cre-dependent reporter mice. The Cre recombinase expression was previously visualized by *LacZ*, a β-galactosidase reporter gene inserted in the ROSA26 locus, that is expressed only

* Correspondence: hidokano@sc.itc.keio.ac.jp
[1]Department of Physiology, Keio University School of Medicine, Shinjuku-ku, Tokyo 160-8582, Japan
Full list of author information is available at the end of the article

after the loxP-flanked intervening sequence is excised by Cre [17]. Once a specific promoter is activated, the cell is indelibly tagged with β-galactosidase. This kind of transgenic mouse is useful for monitoring the transient activation of various promoters, including the NC-specific promoter. Recently, mouse strains expressing a fluorescence-based reporter upon Cre-mediated conditional gene deletion have been developed for prospective cell sorting or direct observation without fixation [18]; the CAG-CAT-EGFP reporter transgenic mouse strain expresses enhanced green fluorescent protein (EGFP) when the loxP-flanked CAT gene located between the modified chicken β-actin promoter (CAG promoter) and the EGFP gene [18] is excised with Cre. In previous studies, we have used mice that enable Cre/loxP-mediated cell labeling with *LacZ* or EGFP to analyze the NC lineage and to trace NC cells after their migration and differentiation [5,19-21].

However, for specific gene regulation analysis, transgenic or knock-in mouse lines that express a specific gene profile *in vivo* are more useful, because the reporter gene is expressed only while the specific promoter or enhancer is active, and ceases when the promoter becomes inactive. Reporter mice have recently been developed to evaluate cell-type specification and maturation in the oligodendroglial lineage; these are the 2'-3'-cyclic nucleotide 3'-phosphodiesterase (*CNP*)-EGFP and myelin proteolipid protein (*PLP*)-EGFP transgenic mouse lines [22,23]. The *CNP*-EGFP transgenic mouse, in which the CNP promoter controls EGFP expression, has been used for the prospective identification of live oligodendroglial cells both *in vivo* and *in vitro* [23]. The *PLP*-EGFP transgenic mouse, in which EGFP expression is driven by the mouse *PLP* gene promoter, has also been developed for investigating oligodendrocyte lineage cells without fixation and immunostaining [22].

Sox10 expression is closely related to NC-lineage cells. The $Sox10^{LacZ/+}$ [24], *Sox10*-rtTA [25], and *Sox10*-Cre [26] mouse lines have all been reported to label NC cells and oligodendrocytes. $Sox10^{LacZ/+}$ [24], a mutant mouse targeting *Sox10*, was generated by replacing the open reading frame of *Sox10* with *lacZ* sequences. The $Sox10^{LacZ/+}$ mutation causes haploinsufficiency, in which even heterozygous pups have the phenotype found in mice with a spontaneous mutation in the *Sox10* allele. Although *LacZ* expression in this knock-in strain faithfully reflects the endogenous Sox10 expression, it is difficult to observe normal developmental behavior in the labeled cells because of the abnormal and pathological condition of the $Sox10^{LacZ/LacZ}$ homozygous mice [24]. Another unique reporter strain is the *Sox10*-rtTA knock-in mouse [25], in which a variant of the reverse tetracycline-controlled transactivator (rtTA) is inserted into the genomic *Sox10* locus, and the mice are crossed with the doxycycline-dependent *LacZ* reporter line. This strain correctly recapitulates endogenous Sox10 expression in the NC and its derivatives, and also in oligodendrocytes. This inducible transgenic system is limited in its range of analysis, because the reporter gene expression is temporary and requires X-gal staining [25]. The *Sox10*-Cre transgenic mouse strain, designated as the S4F:Cre mouse, when crossed with the reporter line strain Rosa-*LacZ*, identifies cells expressing Sox10, including NC-derived cells, oligodendrocytes, and cells in the ventral neural tube [26]. These strains are powerful tools for tracing the progeny of Sox10-expressing cells in analyses of NC cell migration and oligodendroglial differentiation. However, permanent reporter gene expression does not permit the real-time analysis of Sox10 expression. To overcome these limitations, we generated a new *Sox10*-Venus transgenic mouse, and confirmed that it enables the normal behavior of Sox10-expressing cells to be observed *in vivo*.

Results

Sox10-Venus BAC transgenic mouse generation

To examine the Sox10 expression profile *in vivo*, we took advantage of the bacterial artificial chromosome (BAC) transgenic strategy where entire regulatory machinery for a given gene expression might be covered with a single BAC clone. In short, we modified a 225.6 kb-sized BAC clone *RP24-85O14* by means of homologous recombination to harbor the coding sequence of the fluorescent Venus protein [27] in-frame to the *Sox10* translation initiation codon (ATG) that locates at the middle portion of the clone. This construct yielded seven BAC transgenic founders expressing Venus and we hereafter analyzed the complete expression profile in a particular transgenic founder with the brightest illumination.

First, we evaluated the distribution of Venus fluorescence at each developmental stage of the *Sox10*-Venus mouse embryo. Venus fluorescence in classical NC lineage tissues was directly visible from outside the embryo by using an epifluorescence microscope and a UV light. At embryonic day 11.5 (E11.5 d), Venus green fluorescence was particularly intense in the dorsal root ganglia (DRG) and the trigeminal ganglia (cranial nerve V) (Figure 1A). We observed that Venus fluorescence was not limited to classical NC lineage tissue, but was also observed in non-NC tissues, including the otic vesicle. This is consistent with previous studies in which *in situ* hybridization revealed endogenous Sox10 expression in otic vesicle cells [28,29], which are the primitive state of the vestibulocochlear nucleus (cranial nerve VIII). In the facial area of the E11.5 d embryo, aggregated green cells were observed among scattered Venus-positive cells (Figure 1B). The intensity and resolution of the Venus fluorescence allowed

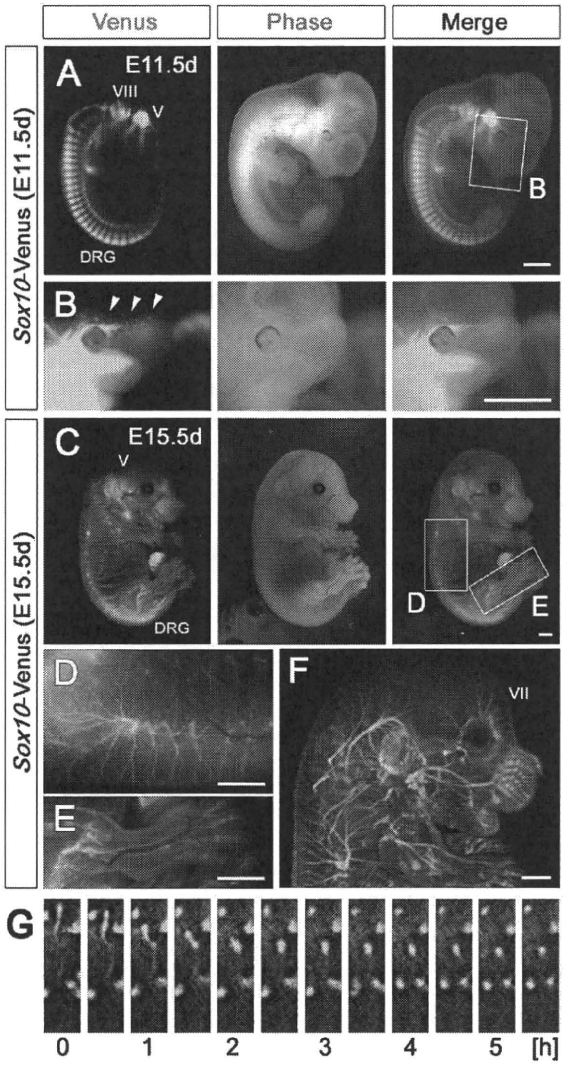

Figure 1 The novel *Sox10*-Venus transgenic mouse strain. The *Sox10*-Venus BAC transgenic mouse strain was generated to investigate the Sox10 expression profile *in vivo*. (A) Venus could be detected in NC lineage tissues, including the DRG and trigeminal ganglia, in E11.5 d mice. Sox10$^+$ cells that were not NC-derived, including cells in the otic vesicle, could also be visualized with Venus. (B) High-intensity fluorescence enabled us to observe a migration stream at the single-cell level, from outside the embryo. (C) At E15.5 d, deep-tissue Venus fluorescence decreased. At this age, migrating Venus$^+$ cells and the network formation of Venus$^+$ cells in the superficial skin layer could be traced. (D) The posterior branches of the spinal nerve were clearly visualized with Venus$^+$ Schwann cells, along with peripheral nerve fibers. (E) In the hind limb, the peripheral nerve and vascular network formations were clearly outlined. (F) The peripheral neural network mainly derived from cranial nerve VII could be visualized with three-dimensional reconstruction with an Olympus MVX-CSU microscope. (G) Time-lapse imaging of the front facial area of embryonic *Sox10*-Venus mice clearly showed individual Venus$^+$ cell movement (also shown in movies in Additional Files 2 and 3). (B) and (D, E) are high-magnification images of the indicated areas in Figures (A) and (C), respectively. Cranial nerves V, trigeminal nerve; VII, facial nerve; VIII, vestibulocochlear nerve, Scale bars; (A-F) 1.0 mm.

us to observe single cells in a pattern suggestive of the NC cell rostral migration process (arrowheads in Figure 1B). As development proceeded from E11.5 d to E15.5 d, Venus fluorescence from the DRGs and nuclei of the cranial nerves located in deep tissues gradually decreased, due to the thickening dermal layer (Figure 1A, C, and Additional file 1A - 1C). However, migrating Venus$^+$ cells in the superficial layer of the embryonic skin were now detectable from outside the body. Venus fluorescence was observed in the Schwann cells of the neural network stemming from the spinal nerve's posterior branches, and in peripheral sensory nerve fibers (Figure 1D). In the hind limb, the peripheral nerve network and the adjacent vascular network were visible (Figure 1E). Three-dimensional reconstructions of the peripheral nerve fibers displayed the entire neural network in the craniofacial area, which

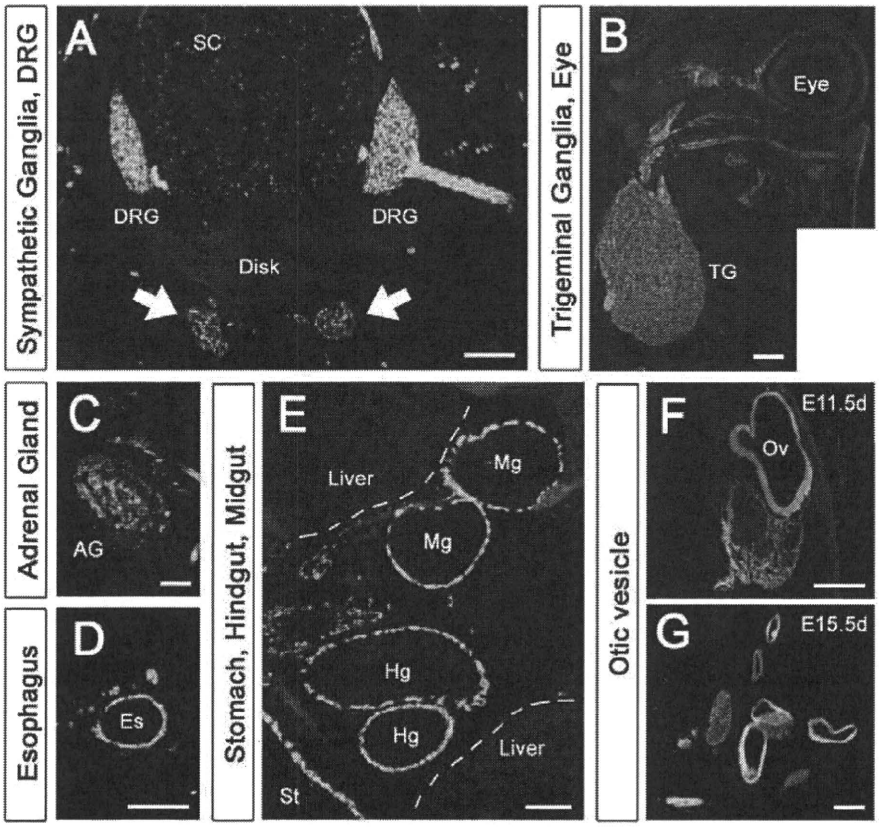

Figure 2 Venus expression in neural crest lineage tissues and in otic vesicle observed without immunostaining. The distribution of Venus$^+$ cells in *Sox10*-Venus mice was evaluated in embryonic-stage cryosections. Venus fluorescence was directly observed without immunostaining. (A) On the thoracic region of an E15.5 d axial section, Venus$^+$ cells were localized to the DRG and its central and peripheral branches. In the spinal cord, Venus$^+$ cells were broadly localized to both the gray matter and the white matter. Venus$^+$ sympathetic ganglion cells were also found at the ventral side of the vertebral body (arrows). (B) In an E15.5 d horizontal section of the cranial area, Venus$^+$ cells concentrated and formed the trigeminal ganglia (the nucleus of the V cranial nerve) and its first branch, the ocular nerve, also visualized by Venus. (C) Venus$^+$ cells were randomly localized in the E15.5 d adrenal gland. (D) NC-derived enteric ganglion cells were seen originating from the XII cranial nerve (Nervous Vargus) and migrating in an oral to anal direction in the alimentary tract. (D-E) On the lumbar level axial section, Venus$^+$ cells were captured in the esophagus, stomach, midgut, and hindgut in the stream of their migration. (F-G) The primary structure of the inner ear, designated as the otic vesicle, also expresses Venus in the embryonic period. The otic vesicle is not NC-derived, but expresses Sox10. SC, spinal cord; TG, trigeminal ganglia; AG, adrenal gland; Es, esophagus; St, stomach; Hg, hindgut; Mg, midgut; Ov, otic vesicle. Scale bars (A-C, E) 100 μm, (D, F-G) 50 μm.

was mainly derived from the branches of the facial nerve (cranial nerve VII) (Figure 1F).

Observing the behavior of individual *Sox10*-Venus cells

The intensity and resolution of the Venus fluorescence in the new *Sox10*-Venus mice led us to evaluate whether it was possible to monitor the behavior of individual cells. Time-lapse imaging *ex-vivo* in skin explants from E14.5 d *Sox10*-Venus embryos was first performed using an epifluorescence microscope. Within this experimental setup, it was easy to detect and follow the movements of single cells (Figure 1G and the movie in Additional File 2). As Sox10 is expressed in deep tissues during the early stages of development, we next examined whether it would be possible to observe Venus fluorescence in whole *Sox10*-Venus embryos. Whole embryos at E10.5 d were observed using a confocal microscope, and followed over time. Time-lapse imaging of the front facial area allowed us to monitor the migration of several Venus$^+$ cells within the embryo over a duration of several hours. We were also able to observe the shape dynamics of individual migrating cells (movie in Additional File 3).

Venus fluorescence in frozen sections of *Sox10*-Venus mice

To confirm the Venus$^+$ cell distribution, we prepared cryosections of *Sox10*-Venus mice from each embryonic stage and observed the Venus fluorescence directly, without any antibody staining or enhancement procedure

(Figure 2). In axial sections of the thoracic region of E15.5 d mouse embryos, Venus fluorescence was intense in the DRG and its proximal and peripheral branches (Figure 2A). Venus$^+$ cells were diffusely present throughout the spinal cord. Some ganglion cells were positive for Venus (Figure 2A, arrows) in the sympathetic ganglia located at the ventral side of the vertebral disc. In horizontal cranial sections from E15.5 d *Sox10*-Venus embryos, large numbers of Venus$^+$ cells accumulated to form the trigeminal ganglia (cranial nerve V) (Figure 2B). Venus was highly expressed in the ocular nerve, which is the first branch of the trigeminal nerve. Venus$^+$ cells were randomly distributed in the E15.5 d adrenal gland, most likely due to the incomplete column structure formation at this stage (Figure 2C). In the alimentary tract, Venus$^+$ enteric ganglion cells originating from the vagal nerve (cranial nerve XII) were found migrating in a rostrocaudal direction through the esophagus, stomach, midgut, and hindgut (Figure 2D and 2E). All of these tissues are well-known NC derivatives, demonstrating that the Venus fluorescence observed in the *Sox10*-Venus mice is consistent with known NC cell localization and differentiation [1-3,5]. In the otic vesicle, which is the primary structure of the inner ear nerve, cells continuously expressed Venus throughout the embryonic period (Figure 2F and 2G). The otic vesicle is not a NC derivative, but Sox10 protein expression in otic vesicle cells during the embryonic stage has been reported [28,29].

Cell type evaluation of the Venus$^+$ cells in *Sox10*-Venus mice

To verify that the Venus expression correctly reflects the endogenous expression of the Sox10 protein *in vivo*, we performed immunohistochemistry of E11.5 d to postnatal 1-week-old (P1 w) whole mouse frozen sections. Without exception, in all the tissues and stages examined, all the Sox10-positive cells expressed Venus. In addition to Sox10 immunostaining, we also examined cell-type-specific markers in NC-derived and Sox10$^+$ tissues. The enteric ganglion cells in the alimentary tract stained with PGP9.5 antibodies. In the esophagus, stomach, midgut, and hindgut, most of the migrated enteric ganglion cells were positive for Venus at E15.5 d (Figure 3A). In the E15.5 d adrenal gland stained for tyrosine hydroxylase (TH), a marker for catecholaminergic cells, TH-positive endocrine cells were positive for Venus (Figure 3B). In the early embryonic (E11.5 d) DRG, all Hu-positive sensory neurons were co-labeled with Sox10 and Venus (Figure 3C). These observations confirmed that *Sox10*-Venus is a useful reporter strain, in which Venus expression faithfully reflects the endogenous Sox10 *in vivo* expression.

Loss of Venus-fluorescence correlates with the shutdown of endogenous Sox10 expression

To evaluate the on/off switching of reporter gene activity in *Sox10*-Venus mice, we verified the Sox10 expression with immunohistochemistry, and examined its correlation with Venus fluorescence. At the late embryonic stage of E15.5 d, the loss of Sox10 expression in Hu-positive DRG neurons coincided with a dramatic decrease in Venus fluorescence, compared to the early embryonic stage (Figure 3C and 3D). A similar phenomenon was observed in embryonic sympathetic ganglia: most of the TH$^+$ neurons were Venus$^+$ in the early embryonic stage, while TH$^+$ neurons in the late embryonic stage lost both Venus and Sox10 expression (Figure 3E and 3F).

The prompt on/off switching of reporter gene activity is an important characteristic of this transgenic mouse strain. In mice in which the NC lineage is labeled, such as the *Wnt1*-Cre/CAG-CAT-EGFP double transgenic mouse, NC progeny expressing Cre are indelibly labeled with the reporter gene. At the late embryonic stage of E15.5 d, neurons in the DRG and sympathetic ganglia of *Wnt1*-Cre/CAG-CAT-EGFP mice were still labeled with EGFP fluorescence even though endogenous Sox10 expression had already diminished (Additional file 4). In contrast, the sensitive on-off switching of the Venus-fluorescent reporting makes the *Sox10*-Venus mouse an accurate, real-time reporter strain.

Identification of Venus$^+$ cells in the intact embryonic spinal cord

Previous reports have suggested that Sox10 is expressed in oligodendrocyte progenitor cells (OPCs) and mature oligodendrocytes [24-26]. We examined the identity of the Venus$^+$ cells observed in the ventral region of the intact embryonic spinal cord of *Sox10*-Venus mice by immunohistochemistry. The Venus$^+$ cells were negative for the pan-neuronal marker Hu (Figure 4A), but positive for the oligodendroglial-lineage markers GSTπ and Olig2 (Figure 4B and 4C). Therefore, in the spinal cord of the embryonic *Sox10*-Venus mouse, Venus labels oligodendroglial-lineage cells without distinction as to their degree of maturation.

Venus$^+$ cells in the intact and injured spinal cords of adult *Sox10*-Venus mice

To examine the phenotype of Venus$^+$ cells in intact and injured spinal cords of *Sox10*-Venus mice, we first observed changes in the Venus$^+$ cells over time (Figure 5A - C). After spinal cord injury (SCI), there was a sharp drop in the number of Venus$^+$ cells, followed by a gradual accumulation around the lesion epicenter at later stages after the injury.

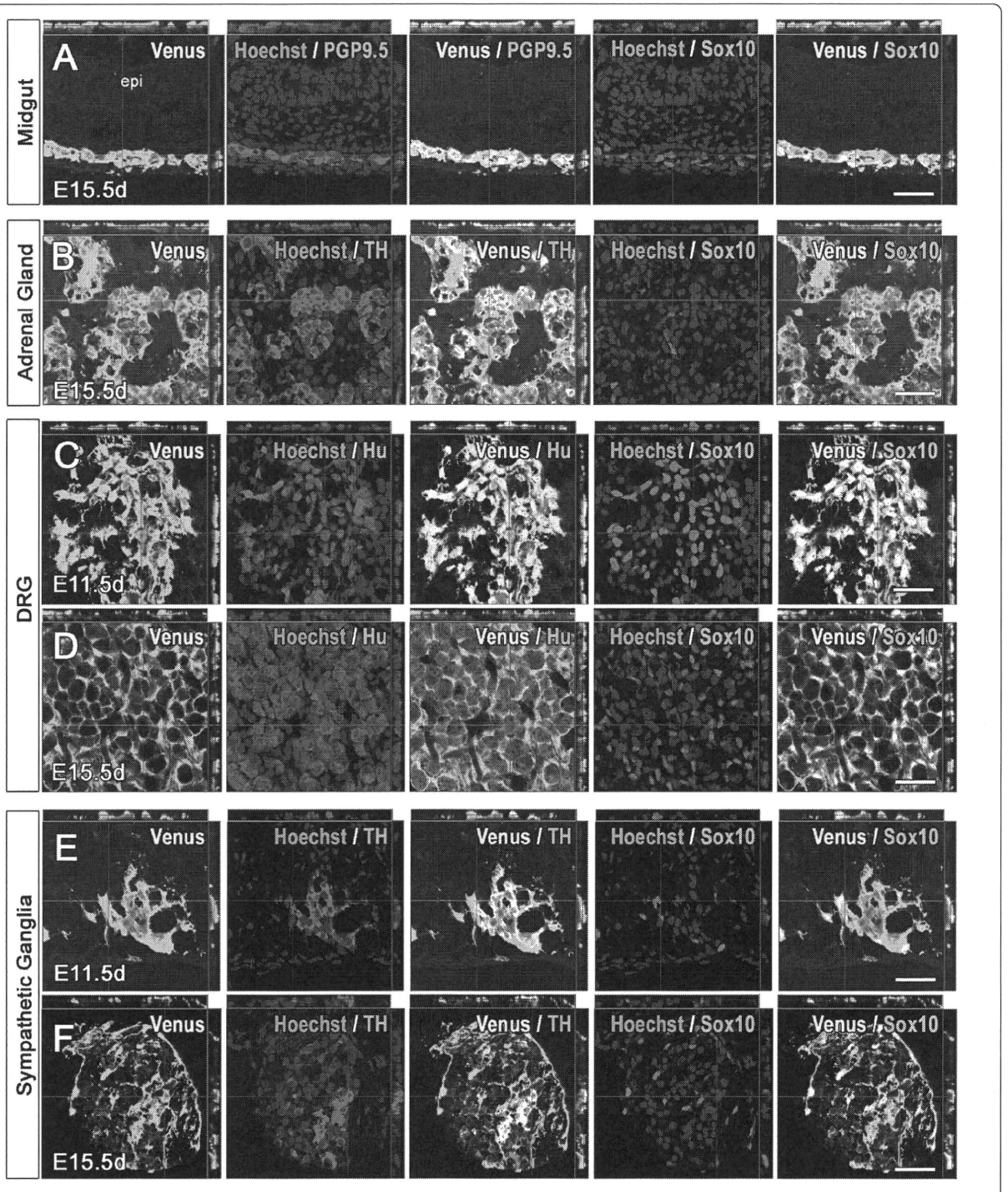

Figure 3 Venus expression faithfully reflects endogenous Sox10 expression. Immunohistochemistry was used to confirm the *in vivo* co-localization of Venus with specific cell-type markers in *Sox10*-Venus mice. (A-F) All Sox10-positive cells were also positive for Venus; no ectopic Venus expression was detected in an entire series of sections. (A) In the E15.5 d alimentary tract, PGP9.5-positive enteric ganglion cells were also positive for Venus. (B) TH-positive endocrine cells in the E15.5 d adrenal gland were invariably positive for Venus. (C-D) While all Hu-positive early embryonic DRG neurons expressed endogenous Sox10 and Venus protein at E11.5 d, mature DRG neurons lost the Sox10 and Venus expression simultaneously at E15.5 d, and $Sox10^+$ satellite cells became positive for Venus. (E-F) In the embryonic sympathetic ganglia, all the TH^+ neurons were also $Venus^+$ at E11.5 d, whereas TH^+/$Venus^-$ cells appeared at E15.5 d. Hu^+, terminally differentiated neuron; $PGP9.5^+$, enteric ganglion cell; TH^+, adrenal gland endocrine cells and sympathetic ganglion neurons; epi, epithelium. Scale bars (A-F) 50 μm.

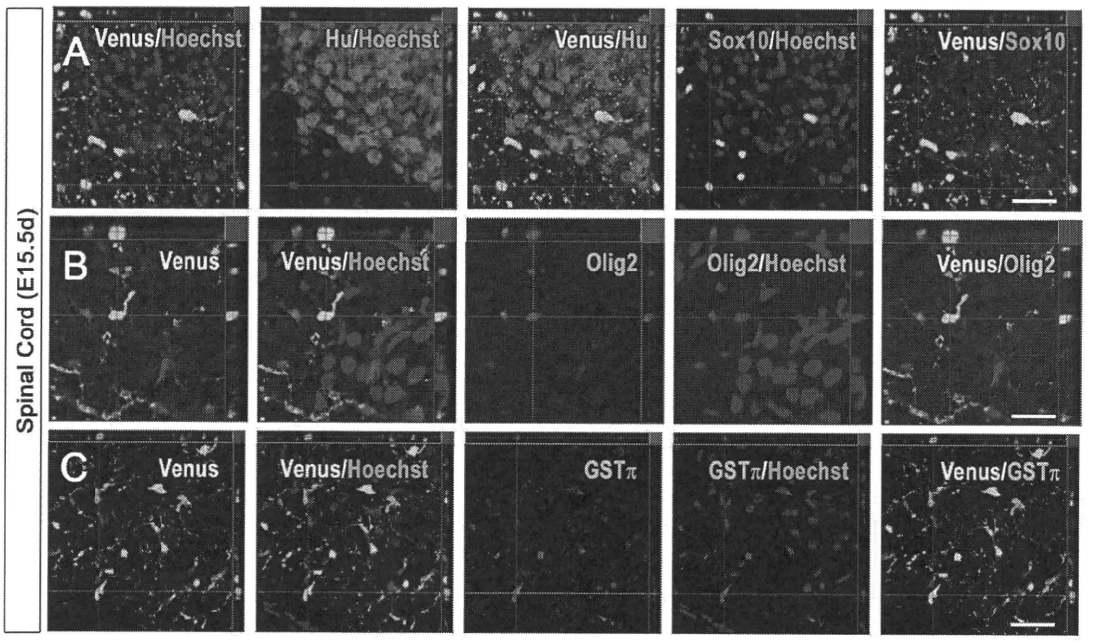

Figure 4 *Sox10*-Venus$^+$ cells in the intact embryonic spinal cord. Immunohistochemical analysis of Venus$^+$ cells in the intact embryonic spinal cord of *Sox10*-Venus mice. (A) Venus fluorescence did not colocalize with the pan-neuronal marker Hu in the ventral area of *Sox10*-Venus mice. (B-C) These Venus$^+$ cells expressed the oligodendroglial lineage markers GSTπ and Olig2, showing that the Venus$^+$ cells were OPCs and mature oligodendrocytes. Scale bars; (A-C) 50 μm.

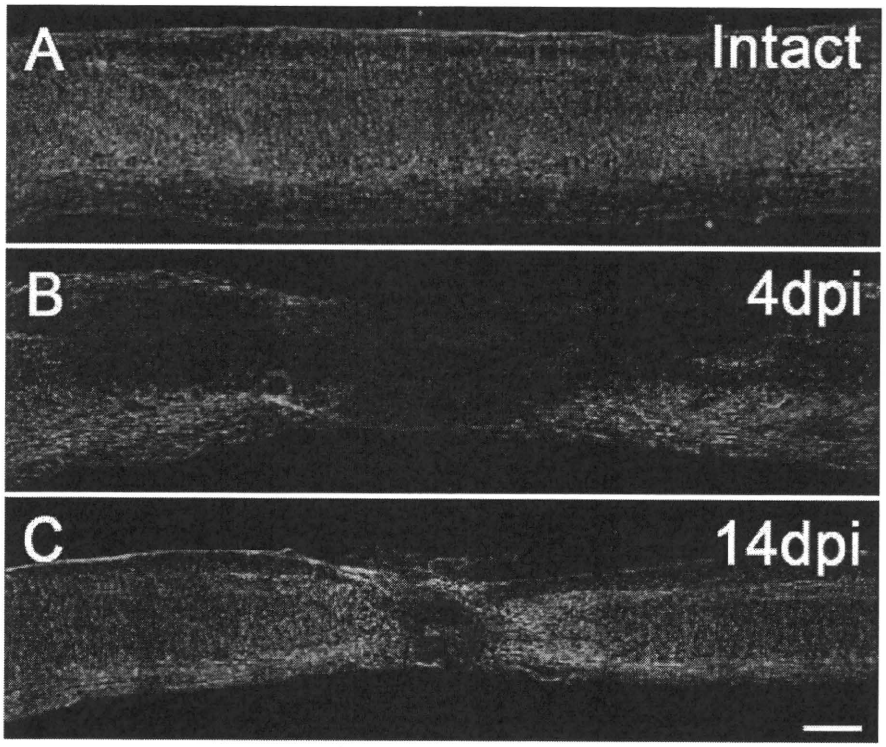

Figure 5 *Sox10*-Venus$^+$ cells actively accumulate at the spinal cord injury site. Venus fluorescence illuminated the behavior of *Sox10*-expressing cells after a spinal cord injury. (A) In an intact adult mouse spinal cord, Venus$^+$ cells were clearly visible in both in the gray and the white matter. (B) In the acute phase of contusive spinal cord injury (4 dpi; days-post-injury), Venus$^+$ cells were absent from the lesion site. (C) In the subacute phase (14 dpi), numerous Venus$^+$ cells were present around the lesion and delineated the lesion epicenter. Scale bars (A-C) 500 μm.

Next, we identified the Venus$^+$ cells in intact and injured spinal cords by immunostaining with various cell markers (Figure 6A - H). In the intact spinal cord, Venus$^+$ cells were easily visualized in both the gray and white matter (Figure 5A), and were mostly positive for GSTπ (Figure 6A). After contusive SCI, Sox10-expressing cells disappeared from the lesion epicenter (Figure 5B). In the acute phase of SCI (4 days-post-injury; 4 dpi), cells positive for NG2 and Venus appeared in the residual white matter (Figure 6B). Although NG2 is also known to stain reactive astrocytes and macrophages [30], the Venus$^+$ cells observed in the injured spinal cord were negative for GFAP (Figure 6D) and CD11b (Figure 6E), indicating that they were Sox10-expressing oligodendrocytes. We also observed Venus$^+$ cells that were positive for PDGFRα, an OPC marker (Figure 6C), suggesting that OPCs also expressed Sox10 in the injured spinal cord.

In the later subacute phase of SCI (14 dpi), numerous Venus$^+$ cells were found in the epicenter and around the lesion site (Figure 5C). Immunohistochemistry revealed that many of the Venus$^+$ cells were positive for S100β, a marker of the Schwann cell lineage, confirming Schwann cell involvement after SCI (Figure 6F). Some of the Venus$^+$ cells had bipolar processes and were positive for p75, suggesting that they were immature Schwann cells (Figure 6G), while a few Venus$^+$ mature Schwann cells were also identified by their P0 expression (Figure 6H). The observation that both immature and mature Schwann cells were Venus$^+$ in the injured spinal cord is consistent with the Schwann cell lineage deriving from the NC.

Comparison of the *Sox10*-Venus strain with other NC reporter mouse strains

The data from several NC reporter mouse lines, such as *Sox10*(S4F)-Cre, *P0*-Cre, *Wnt1*-Cre, and *Ht-Pa*-Cre [5,14,16,26,31,32], have already been published. To compare this body of data to the observations gained from the *Sox10*-Venus mouse, the embryonic expression patterns of various NC-derived tissues are summarized for each strain in Table 1. At the early embryonic period (E11.5 d - E12.5 d), the reporter gene activity of all the mouse strains was quite similar. All the strains demonstrated reporter gene activity in numerous NC-lineage tissues, including the DRG, sympathetic ganglia, melanoblasts, enteric nervous system, superior/jugular ganglion, aorta, and craniofacial mesenchyme. All the strains also showed reporter expression in the otic vesicle, which does not originate from the NC.

Regarding the differences in these reporter strains, CNS myelinating glial cells were not labeled in the *P0*-Cre, *Wnt1*-Cre, and *Ht-Pa*-Cre strains; they were only labeled in the *Sox10*-related strains *Sox10*-Venus and *Sox10* (S4F)-Cre. In the brain and spinal cord, the labeling of oligodendroglial cells and OPCs in the *Sox10*-Venus and *Sox10*-Cre mice reflected the endogenous Sox10 expression in these cells, since they are not derived from the NC. The peripheral nerve network in developing limbs consists of nerve fibers and their associated Schwann cells, which are both derived from the NC. Although the *LacZ* expression in the developing limb was ambiguous in the *Sox10*(S4F)-Cre/Rosa-*LacZ* mouse [26], the Venus fluorescence observed in the same region with the *Sox10*-Venus mouse clearly originated from the Schwann cells (Figure 1E).

Discussion

In this study, we developed and characterized the *Sox10*-Venus BAC transgenic mouse. Analysis of the early embryonic stages showed that not only NC lineage cells, but also oligodendroglial cells were clearly labeled with high-intensity Venus fluorescence (Figure 1 and 2). Compared to other published transgenic and knock-in reporter mouse strains, the *Sox10*-Venus mouse has advantages that make it invaluable for future studies.

The mice with NC-lineage tracing *Wnt1*-Cre, *P0*-Cre, and *Ht-PA*-Cre, crossed with those with Cre/loxP-mediated cell labeling, Rosa-*LacZ* and CAG-CAT-EGFP, can be used only for analyzing cell lineage or migration, because the target cells are irreversibly labeled [5,14-20]. Although *Sox10*-Venus also labels NC-lineage cells, the fast on/off switching of Venus fluorescence is tightly correlated with endogenous Sox10 expression. Similarly, the reporter gene activity in *CNP*-EGFP and *PLP*-EGFP mice, which are transgenic mice that label oligodendroglial-lineage cells, truly reflects the *in vivo* expression of specific genes driven by specific promoters or enhancers. The transgenic system of the *Sox10*-Venus mouse is quite similar to these; however, the Venus fluorescence is brighter and more intense than EGFP fluorescence.

Although reporter gene activity occurs in NC cells and oligodendrocytes in all *Sox10* reporter mouse lines, i.e., *Sox10*$^{LacZ/+}$, *Sox10*-rtTA, *Sox10*-Cre strains [24-26], and the new *Sox10*-Venus strain, each line has advantages and disadvantages. *LacZ* knock-in *Sox10*$^{LacZ/+}$ heterozygous pups are prone to spontaneous mutation phenotypes due to haploinsufficiency. Also, to observing the *LacZ* expression in *Sox10*$^{LacZ/+}$ mice requires additional visualization procedures, making live cell imaging difficult. The *Sox10*-rtTA knock-in crossed with the inducible TRE-*LacZ* transgenic is unique, but the reporter expression is transient and does not fluoresce, making it difficult to observe directly. The *Sox10*-Cre/CAG-CAT-EGFP double transgenic mouse traces both NC and oligodendrocyte progeny, since it reports past as well as ongoing Sox10 expression. With this double transgenic mouse, it is possible to carry out cell sorting or live imaging.